Journal of Molecular Structure 1043 (2013) 43–51

Contents lists available at SciVerse ScienceDirect

Journal of Molecular Structure

journal homepage: www.elsevier.com/locate/molstruc

Structure, absorption and fluorescence of (bi)thiophene substituted methylidene-pyrrolinones

Zdeněk Eliáš [a,b,*], Stanislav Luňák Jr. [a], Jan Vyňuchal [b], Antonín Lyčka [c,d], Zdeňka Padělková [a], Radim Hrdina [a]

[a] Faculty of Chemical Technology, University of Pardubice, Studentská 95, CZ-532 10 Pardubice, Czech Republic
[b] Synthesia a.s., Pardubice, Semtín 103, CZ-532 17 Pardubice, Czech Republic
[c] Research Institute for Organic Syntheses (VUOS), Rybitví 296, CZ-533 54 Pardubice 20, Czech Republic
[d] University of Hradec Králové, Faculty of Education, Rokitanského 62, CZ 500 03 Hradec Králové 3, Czech Republic

HIGHLIGHTS

- Methylidene-pyrrolinones with heterocyclic rings were synthesized and compared with aromatic ones analogues.
- Structures were estimated by DFT and proved by X-ray diffraction in two cases.
- *N*-methylated derivatives show solid-state fluorescence.

ARTICLE INFO

Article history:
Received 3 February 2013
Received in revised form 26 March 2013
Accepted 26 March 2013
Available online 2 April 2013

Dedicated to Professor Miloš Nepraš in occasion of his 80th birthday

Keywords:
Absorption
Fluorescence
X-ray diffraction
Density functional theory

ABSTRACT

Four thiophene and bithiophene substituted methylidene-pyrrolinones were synthesized and their absorption and fluorescence properties were compared with previously reported behavior of their phenyl and biphenyl substituted analogues. Their structures were estimated theoretically by density functional theory (DFT) and proved by X-ray diffraction in two cases. Thiophene derivatives show a considerable bathochromic shifts in absorption with respect to phenyl analogues, in accordance with theoretical predictions based on time dependent DFT. Conjugation extension caused a bathochromic shift in absorption, too. All compounds show fluorescence in low temperature solvent glass, while only one bithiophene substituted derivative fluoresce weakly in room temperature solution. Three of four *N*-methylated derivatives show strong yellow, orange and red solid-state fluorescence. An ability of solid-state fluorescence was correlated with nearest neighbor out-of-plane interactions in crystal.

1. Introduction

Solid-state (ss) fluorescence of organic conjugated compounds is of general interest because of its use in organic light-emitting diodes and field-effect transistors, solid-state lasers and luminescent sensors [1]. Except the intramolecular competitive radiationless processes given by Jablonski diagram, the intermolecular ones (like electron and energy transfer [1] or triplet fission [2]) must be taken into account. Consequently, the relation between crystal structure and fluorescence ability has to be considered in ss fluorophores research. The transfer processes are usually correlated with local nearest-neighbor interactions [3–7], nevertheless sometimes this model is insufficient and the global properties like crystal rigidity may play crucial role [8]. The relation between the ability of a molecule to fluoresce in solution and in crystal is not straightforward. The molecules strongly fluorescent in solution usually save this property in solid, if the strong intermolecular interactions like π–π stacking are absent [9,10]. On the other hand, a lot of compounds non- or weakly fluorescent in solution show aggregation- or crystallization-induced emission enhancement [11]. One of the possible mechanisms of such enhancement (restriction of excited state intramolecular rotation) is probably responsible for ss fluorescence of aryl-methylidene-pyrrolinones, reported by our group [12]. Multicolor emission obtained by substituent tuning forms one of the challenges in the area of ss emitters [1]. We have recently shown, that the variations of peripheral substituents on diketo-pyrrolo-pyrrole (DPP) chromophore can tune the ss fluorescence maximum in a broad range over 200 nm in a visible and near-infrared region (568–784 nm) [13]. On the other hand, vinylene and phenylene-vinylene conjugation extension of phenyl-methylidene-pyrrolinones, coming from the same precursor as

---

* Corresponding author at: Faculty of Chemical Technology, University of Pardubice, Studentská 95, CZ-532 10 Pardubice, Czech Republic. Fax: +420 466823900.

E-mail address: elias.zd@seznam.cz (Z. Eliáš).

0022-2860/$ - see front matter © 2013 Elsevier B.V. All rights reserved.
http://dx.doi.org/10.1016/j.molstruc.2013.03.055

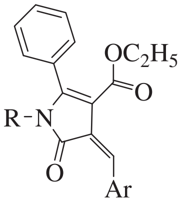

Ar	R	Compound
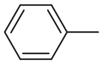	H	**1**
	CH_3	**1m**
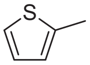 	H	**2**
	CH_3	**2m**
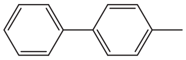	H	**3**
	CH_3	**3m**
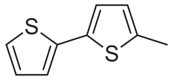 	H	**4**
	CH_3	**4m**

Scheme 1. Compounds under study.

unsymmetrical DPPs (i.e. pyrrolinone ester), lead only to relatively narrow region of ss fluorescence maxima (561–630 nm) [12]. Thus the main aim of the presented study was to modify the structure of aryl-methylidene-pyrrolinones to shift the ss fluorescence maxima to longer wavelengths.

Inspired by that fact, that a substitution of 3,6-phenyl rings of DPP chromophore by oligothiophenes brings a higher bathochromic shift in absorption and fluorescence [14] compared to conjugation extension based solely on hydrocarbons [15], we have synthesized compounds **2** and **4** (Scheme 1) as heteroanalogues of previously reported compounds **1** and **3** [16]. Furthermore, their better soluble *N*-methyl derivatives **2m** and **4m** were synthesized. Comparable compound **1m** was reported in our previous study [12] and the compound **3m** was newly synthesized to complete the series and to cover the effect of phenylene conjugation extension in *N*-methylated series. Five new compounds were fully characterized and X-ray diffraction was applied in two cases (**2m** and **4m**), in which the monocrystals of sufficient quality were prepared, in order to confirm the molecular structure and to evaluate the intermolecular interactions in solid state. An effect of heterosubstitution and conjugation extension on experimental absorption spectra was supported by theoretical calculations of excitation energies based on time dependent density functional theory (TD DFT) including the solvent effect by polarized continuum model (PCM). The fluorescence ability was studied in solution, in low temperature solvent glass and in polycrystalline solid-state.

2. Experimental and theoretical procedures

2.1. Syntheses and analyses

Compounds **2** and **4** were synthesized by piperidine catalyzed condesation of 2-thiophene and 2-bithiophene carboxaldehydes with pyrrolinone ester (ethyl 5-oxo-2-phenyl-4,5-dihydro-1*H*-pyrrole-3-carboxylate) as reported previously [12,16]. Methyl iodide was used an agent in *N*-methylation of **2**, **3** and **4** to form **2m**, **3m** and **4m** according to Ref. [12]. All compounds arose solely as *Z* isomers on newly formed exocyclic double bond as confirmed by $^3J(^{13}C, ^1H)$ coupling constants on methylidene proton. All compounds show *s-trans* conformation of carboxy ester group according to methyl and methylene ^1H NMR chemical shifts [12].

2.1.1. Synthesis of ethyl (4Z)-5-oxo-2-phenyl-4-(thiophen-2-ylmethylidene)-4,5-dihydro-1H-pyrrole-3-carboxylate (2)

Toluene (25 ml), ethyl 5-oxo-2-phenyl-4,5-dihydro-1*H*-pyrrole-3-carboxylate (pyrrolinone ester; 1.25 g; 5.42 mmol) and thiophene-2-carbaldehyde (0.61 g; 5.42 mmol) were added into round bottom flask. The reaction mixture was heated under reflux for 4 h in the catalytic presence of piperidine (c. 1.5 ml). Solid portion was separated in the reaction mixture after 20 min of heating and thus toluene (10 ml) was added in order to improve stirring. The product was filtrated and dried. It was obtained with 82% yield. The melting point was 214–216 °C. Elemental analysis: Calculated: C (66.44), H (4.65), N (4.30), S (9.85) Found: C (66.36), H (4.54), N (4.27), S (9.93). MS analysis M = 325. Positive-ion MS: *m*/*z* 326 [M+H]+, 100%.

2.1.2. Synthesis of ethyl (4Z)-5-oxo-2-phenyl-4-(2,2′-bithiophen-5-ylmethylidene)-4,5-dihydro-1H-pyrrole-3-carboxylate (4)

Toluene (15 ml), pyrrolinone ester (0.63 g; 2.7 mmol) and 2,2′-bithiophene-5-carbaldehyde (0.6 g; 2.7 mmol) were added into round bottom flask. The reaction mixture was heated under reflux for 6 h in the catalytic presence of piperidine (c. 0.75 ml). The reaction was monitored by TLC (n-hexane:acetone 3:2). Toluene (10 ml), pyrrolinone ester (0.53 g) and piperidine (0.5 ml) were added and the mixture was heated under reflux next 6 h due to presence of starting aldehyde. Then more pyrrolinone ester (0.25 g) and toluene (10 ml) were added and reaction mixture was heated for the following 6 h under reflux. The product was filtrated and dried. It was obtained with 95% yield. The melting point was 224–226 °C. Elemental analysis: Calculated: C (64.84), H (4.20), N (3.44), S (15.74), Found: C (64.83), H (4.17), N (3.51), S (15.51). MS analysis M = 407. Positive-ion MS: *m*/*z* 408 [M+H]+, 100%.

2.1.3. General procedure for the synthesis of methylated derivatives

DMF (60 ml), starting non-methylated compound (2.15 mmol) and potassium carbonate (3 mmol) were given to the three-necked

Table 1
DFT dihedral angles and relative energies (ΔE) of isomers/conformers of compound **2**. α, β and γ describe the C—C=C—C(=O), C=C—C(OEt)=O and C=C—C=C(Th) dihedral angles, respectively, i.e. *Z*/*E* isomers on C=C and *s-trans*/*s-cis* conformers on C—C leading to ethyl ester and thiophene groups.

Isomer	Conformer (ester)	Conformer (thiophene)	α (°)	β (°)	γ (°)	ΔE (kcal mol^{-1})
E	*s-trans*	*s-trans*	−171	−142	176	6.510
		s-cis	−177	−137	−10	6.233
	s-cis	*s-trans*	−163	38	−169	6.908
		s-cis	−163	43	25	6.397
Z	*s-trans*	*s-trans*	0	−174	−179	0.000
		s-cis	0	−173	1	0.276
	s-cis	*s-trans*	−1	−13	−179	0.859
		s-cis	−1	−15	0	1.130

flask with thermometer and refluxing condenser. After 20 min of stirring was heated to 80 °C and iodomethane (12.9 mmol) was added. The reaction mixture was heated at 80 °C for 2 h. Product was isolated by precipitation to 50 ml distilled water and was filtered off.

2.1.4. Ethyl (4Z)-1-methyl-5-oxo-2-phenyl-4-(thiophen-2-ylmethylidene)-4,5-dihydro-1H-pyrrole-3-carboxylate (**2m**)

Product was obtained with 90% yield. The melting point was 125–128 °C. Elemental analysis: Calculated: C (67.27), H (5.05), N (4.13), S (9.45) Found: C (67.09), H (4.89), N (4.08), S (9.36). MS analysis M = 339. Positive-ion MS: *m*/*z* 340 [M+H]+, 100%.

2.1.5. Ethyl (4Z)-4-(biphenyl-4-ylmethylidene)-1-methyl-5-oxo-2-phenyl-4,5-dihydro-1H-pyrrole-3-carboxylate (**3m**)

Product was obtained with 90% yield. The melting point was 125–128 °C. Elemental analysis: Calculated: C (79.20), H (5.66), N (3.42), Found: C (78.53), H (5.49), N (3.37). MS analysis M = 409. Positive-ion MS: *m*/*z* 410 [M+H]+, 100%.

2.1.6. Ethyl (4Z)-4-(2,2′-bithiophen-5-ylmethylidene)-1-methyl-5-oxo-2-phenyl-4,5-dihydro-1H-pyrrole-3-carboxylate (**4m**)

Product was obtained with 92% yield. The melting point was 139–141 °C. Elemental analysis: Calculated: C (65.53), H (4.54), N (3.32), S (15.21) Found: C (65.32), H (4.42), N (3.27), S (14.88). MS analysis M = 421. Positive-ion MS: *m*/*z* 422 $[M+H]^+$, 100%; *m*/*z* 314 $[M+H—C_2H_5OH]^+$.

2.2. Instrumental equipment

The ^{1}H and ^{13}C NMR spectra were recorded on a Bruker Avance II 400 spectrometer (400.13 MHz for ^{1}H, and 100.62 MHz for ^{13}C) in DMSO-d_6. The ^{1}H and ^{13}C chemical shifts were referenced to internal TMS (δ = 0.00). All 2D experiments (gradient-selected gs-COSY, gs-HMQC, gs-HMBC) were performed using manufacturer's software (Topspin 2.1).

The X-ray data for crystals of **2m** (yellow) and **4m** (orange) were obtained at 150 K using Oxford Cryostream low-temperature device on a Nonius KappaCCD diffractometer with Mo Kα radiation (λ = 0.71073 Å), a graphite monochromator, and the φ and χ scan mode. Data reductions were performed with DENZO-SMN [17]. The absorption was corrected by integration methods [18]. Structures were solved by direct methods (Sir92) [19] and refined by full matrix least-square based on F^2 (SHELXL97) [20]. Hydrogen atoms were mostly localized on a difference Fourier map, however to ensure uniformity of treatment of crystal, all hydrogens were recalculated into idealized positions (riding model) and assigned temperature factors $H_{iso}(H) = 1.2\ U_{eq}$ (pivot atom) or of 1.5 U_{eq} for the methyl moiety with C—H = 0.96, 0.97, 0.93 and 0.93 Å for methyl, methylene, vinylidene hydrogen atoms and atoms in aromatic rings, respectively.

Crystallographic data for structural analysis have been deposited with the Cambridge Crystallographic Data Centre, CCDC Nos. 921116 and 921117 for **2m** and **4m**, respectively. Copies of this information may be obtained free of charge from The Director, CCDC, 12 Union Road, Cambridge CB2 1EY, UK (fax: +44 1223 336033; e-mail: deposit@ccdc.cam.ac.uk or http://www.ccdc.cam.ac.uk).

The absorption spectra were recorded at room temperature in DMSO using a Perkin-Elmer Lambda 35 spectrophotometer in 1 cm pathlength quartz cuvettes. A Perkin-Elmer (PE) LS55 was used for measuring fluorescence spectra. Methyltetrahydrofuran (MTHF) was used as a solvent to create an organic frozen glass to measure low temperature fluorescence spectra using a commercial low temperature accessory also from PE. This accessory contains an isolated box filled by liquid nitrogen and the measurements are carried out in a round cuvette (diameter about 1 mm). The solid state luminescence spectra were recorded also on the same instrument equipped with a PE accessory for solid state measurements.

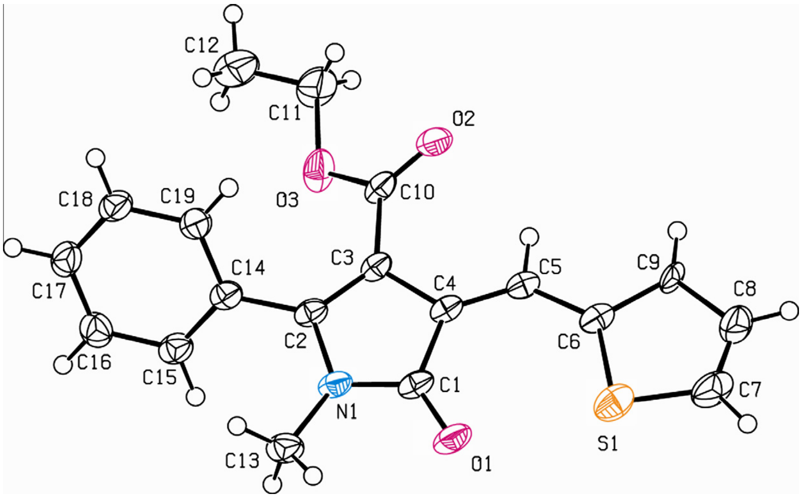

Fig. 1. The molecular structure (ORTEP 50% probability level) of **2m**. Selected interatomic distances (Å); angles and interplanar angle (°): O1 C1 1.230(3), O2 C10 1.202(4), C1 N1 1.375(4), N1 C2 1.407(4), C2 C3 1.364(4), C3 C4 1.463(4), C4 C1 1.477(4), C4 C5 1.355(4), C5 C6 1.431(4), C6 C9 1.478(4), S1 C6 1.726(3), S1 C7 1.672(4); C1 N1 C2 110.6(2), N1 C1 C4 106.8(2), C1 C4 C5 127.9(3), C4 C5 C6 133.6(3), C5 C6 S1 129.0(3) and interplanar angle of phenyl ring *vs.* heterocyclic ring containing amido group is 50.76.

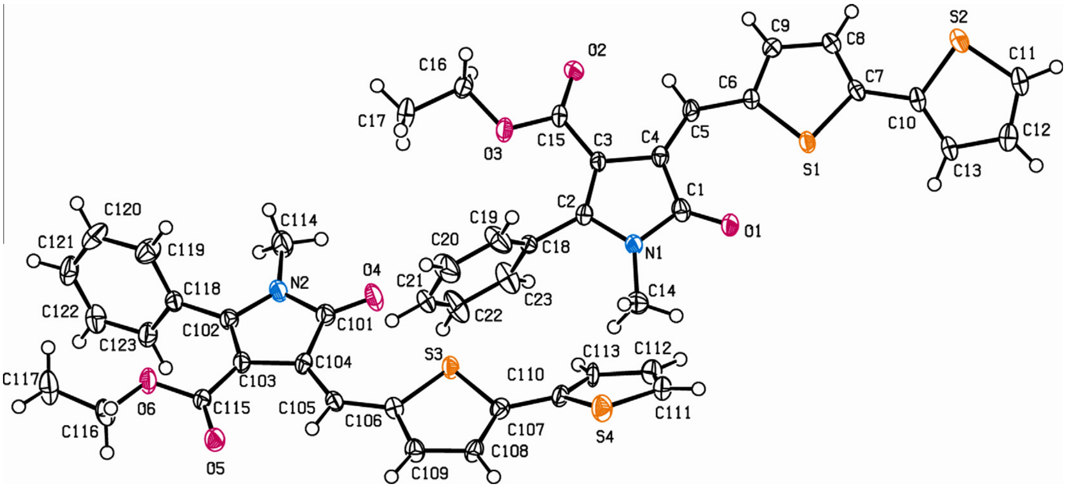

Fig. 2. The molecular structure (ORTEP 50% probability level) of **4m**. Selected interatomic distances (Å); angles and interplanar angles (°): for molecule **a**: O1 C1 1.235(4), O2 C15 1.206(5), C1 N1 1.387(5), N1 C2 1.400(4), C2 C3 1.355(5), C3 C4 1.470(5), C4 C1 1.454(5), C4 C5 1.360(5), C5 C6 1.441(5), C6 S1 1.741(4), S1 C7 1.730(4), C6 C9 1.379(5); C1 N1 C2 109.8(3), N1 C1 C4 106.7(3), C1 C4 C5 128.0(3), C4 C5 C6 132.7(4), C5 C6 S1 128.8(3) and phenyl ring *vs.* heterocyclic ring amido containing 87.82; for molecule **b**: O4 C101 1.218(4), O5 C115 1.204(4), C101 N2 1.387(5), N2 C102 1.391(5), C102 C103 1.355(5), C103 C104 1.466(5), C104 C101 1.481(5), C104 C105 1.351(5), C105 C106 1.438(5), C106 S3 1.742(4), S3 C107 1.733(4), C107 C110 1.453(5), C110 S4 1.727(4), S4 C111 1.705(4); C101 N2 C102 110.4(3), N2 C101 C104 105.9(3), C101 C104 C105 127.2(3), C104 C105 C106 133.9(4), C105 C106 S3 127.9(3) and interplanar angle of phenyl ring *vs.* heterocyclic ring containing amido group is 72.71.

Polycrystalline samples were placed under quartz plate and the emission spectra were recorded using front face geometry.

2.3. Quantum chemical calculations

The theoretical calculation based on DFT were carried out. The ground state geometry was optimized using B3LYP functional in combination with 6-311G(d,p) basis set. TD DFT calculations of excitation energies were carried out with the same xc functional and the broader basis set 6-311+G(2d,p). Solvent effect of dimethylsulfoxide was taken into account through non-equilibrium PCM. The same xc functional, but only 6-311G(d,p) basis set was used for excited state TD DFT optimization of model compounds **1**, **2** and **4** with only hydrogens (not ethyl esters) in positions 3 of pyrrolinone ring. All calculation codes came from Gaussian09W program suite [21].

3. Results and discussion

3.1. Molecular structure

There are two possible isomers of compound **1** and each of them can theoretically exist in two conformational arrangements with respect to an orientation of side carboxy ester group with respect to pyrrolinone ring. Among them *s-trans* conformer is preferred for *Z* isomer and *s-cis* for *E* isomer from sterical reasons [12]. In the case of (bi)thiophene derivatives the third structural (conformational) aspect has to be taken into account – an orientation of thiophene ring, which can be also described by *s-trans* and *s-cis* conformations. Thus the dependence of relative molecular energy on DFT optimized geometry was carried out for all eight possible isomers/conformers of compound **2** (Table 1).

Z isomers of **2** are planar in the area of exocyclic C=C and C—C bonds; the most stable conformer is *s-trans* both on ester and thiophene. The energy destabilization induced by conformational change is almost additive, i.e. 0.27 kcal mol^{-1} per ester group rotation and 0.86 kcal mol^{-1} per thiophene rotation. Distorted *E* isomers are at least 6.23 kcal mol^{-1} less stable, i.e. considerably more than for compound **1** (2.38 kcal mol^{-1}) [12], and their conformational preferences are a bit complicated, as they depend on gentle sterically driven equilibria. The energy difference between the most and the least stable conformers of *Z* isomer is 1.13 kcal mol^{-1}, while only 0.67 kcal mol^{-1} for *E* isomers. Finally, *Z* isomer can be expected as the reaction product in the syntheses of compound **2**, preferably in *s-trans* conformations, while the expected conformation of eventual *E* photoisomer is not so clear, as three of four conformers differ mutually less than 0.28 kcal mol^{-1}. The detailed screening the ground state energy minima with respect to various conformations of compound **4** was not done, but the computed energy difference between *Z* and *E* isomers (both in *s-trans*/*s-trans* arrangements) is 6.685 kcal mol^{-1}, i.e. a destabilization of *E* with respect to *Z* isomer is similar as for compound **2** (6.510 kcal mol^{-1}).

Single crystals of **2m** and **4m** were of sufficient quality for X-ray diffraction techniques. Crystallographic data for **2m**: $C_{19}H_{17}NO_3S$, M = 339.40, monoclinic, $P2_1/c$, $a = 12.0090(8)$, $b = 7.7050(6)$, $c = 17.9859(9)$ Å, $\beta = 90.373(5)°$, $Z = 4$, $V = 1664.19(19)$ Å^3, $D_c = 1.355$ g cm^{-3}, $\mu = 0.211$ mm^{-1}, $T_{min}/T_{max} = 0.952/0.969$; $-12 \leqslant h \leqslant 15$, $-10 \leqslant k \leqslant 9$, $-23 \leqslant l \leqslant 20$; 11,032 reflections measured ($\theta_{max} = 27.15°$), 10,955 independent ($R_{int} = 0.0307$), 2890 with $I > 2\sigma(I)$, 217 parameters, $S = 1.096$, $R1$(obs. data) = 0.0691, $wR2$(all data) = 0.1743; max., min. residual electron density = 1.381, −0.571 eÅ^{-3}.

Crystallographic data for **4m**: $C_{23}H_{19}NO_3S_2$, M = 421.51, triclinic, P-1, $a = 8.6640(6)$, $b = 11.3269(6)$, $c = 21.3571(15)$ Å, $\alpha = 75.581(4)$, $\beta = 86.090(6)$, $\gamma = 80.784(4)°$, $Z = 4$, $V = 2002.8(2)$ Å^3, $D_c = 1.398$ g cm^{-3}, $\mu = 0.291$ mm^{-1}, $T_{min}/T_{max} = 0.924/0.981$; $-11 \leqslant h \leqslant 11$, $-14 \leqslant k \leqslant 14$, $-27 \leqslant l \leqslant 27$; 33,050 reflections measured ($\theta_{max} = 27.4°$), 32,963 independent ($R_{int} = 0.1211$), 5403 with $I > 2\sigma(I)$, 523 parameters, $S = 1.119$, $R1$(obs. data) = 0.0756, $wR2$(all data) = 0.1176; max., min. residual electron density = 0.430, −0.661 eÅ^{-3}.

Compound **2m** (Fig. 1) crystallize in the monoclinic space group $P2_1/c$ with four molecules within the unit cell, on the other hand the compound **4m** crystallizes in the triclinic space group *P*-1 with four molecules within the unit cell and two independent molecules (Fig. 2). In the molecules of both compounds, the interatomic angles inside of central heterocyclic rings confirm that these rings are planar with a high degree of conjugation while the C4—C5 bonds are attributed as a multiple ones. The direct comparison of the structure of **2m** and **4m** with recently obtained and in detail described structure of **1m** [12] with the same central ring can be done.

Table 2

^{1}H and ^{13}C NMR chemical shifts for compounds **2**, **2m**, **3m**, **4** and **4m** in DMSO-D$_6$

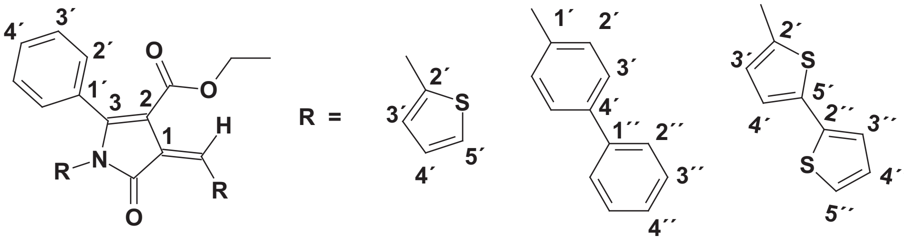

H/C No.	Z-2		E-2		Z-4	
	$\delta(^{1}\mathrm{H})$	$\delta(^{1}\mathrm{H})$	$\delta(^{13}\mathrm{C})$	$\delta(^{13}\mathrm{C})$	$\delta(^{1}\mathrm{H})$	$\delta(^{13}\mathrm{C})$
NH/NCH$_3$	11.07	–	10.96	–	11.12	–
C═O	–	166.6	–	168.6	–	166.7
1	–	123.9	–	125.9	–	123.4
2	–	102.6	–	104.6	–	102.8
3	–	149.6	–	149.2	–	149.5
COO	–	163.2	–	164.2	–	163.2
CH$_2$	4.12	59.5	4.01	60.4	4.13	59.5
CH$_3$	1.08	13.7	0.93	13.4	1.09	13.7
═CHR	8.37	131.0			8.30	130.8
3-1′	–	130.4			-	130.4
3-2′	7.61	129.2			7.62	129.3
3-3′	7.52	127.8			7.52	127.9
3-4′	7.52	130.0			7.52	130.1
R-1′	–	–	–	–	–	–
R-2′	–	137.9			–	136.4
R-3′	7.94	138.0			7.82	139.9
R-4′	7.29	127.7			7.52	124.3
R-5′	7.94	134.4			-	139.9
R-1″	–	–	–	–	–	–
R-2′	–	–	–	–	–	136.7
R-3″	–	–	–	–	7.56	125.5
R-4′	–	–	–	–	7.21	128.8
R-5″	–	–	–	–	7.68	127.2

	Z-2 m		Z-3 m		Z-4 m	
	$\delta(^{1}\mathrm{H})$	$\delta(^{13}\mathrm{C})$	$\delta(^{1}\mathrm{H})$	$\delta(^{13}\mathrm{C})$	$\delta(^{1}\mathrm{H})$	$\delta(^{13}\mathrm{C})$
NH/NCH$_3$	2.95	27.5	2.91	27.7	3.37	27.6
C═O	–	165.2	–	165.2	–	165.3
1	–	121.9	–	127.1	–	121.4
2	–	102.9	–	103.6	–	103.1
3	–	152.1	–	153.4	–	151.9
COO	–	162.8	–	163.3	–	162.8
CH$_2$	3.96	59.1	3.96	59.2	3.97	59.2
CH$_3$	0.88	13.4	0.86	13.5	0.90	13.5
═CHR	8.51	132.0	8.28	140.6	8.44	131.8
3-1′	–	130.6	–	130.7	–	130.6
3-2′	7.49	129.1	a	b	7.50	129.2
3-3′	7.55	128.0	a	b	7.56	128.1
3-4′	7.55	129.4	a	b	7.56	129.5
R-1′	–	–	–	133.4	–	–
R-2′	–	137.8	8.40	132.6	–	136.3
R-3′	7.97	138.6	7.82	b	7.84	140.4
R-4′	7.31	127.8	–	142.0	7.52	124.3
R-5′	8.00	134.9	–	–	–	144.2
R-1″	–	–	–	139.2	–	–
R-2′	–	–	a	b	–	136.6
R-3″	–	–	a	b	7.58	125.6
R-4′	–	–	a	b	7.22	128.8
R-5″	–	–	–		7.69	127.3

[a] 7.80–7.84 and 7.44–7.60 (10H, m).

[b] 132.6, 129.6, 129.1, 129.0, 128.2, 126.8, 126.4 (all ═CH—).

Generally, the experimental geometry of *Z* isomers of **2m** and **4m** is planar on exocyclic carbon–carbon bonds. Both compounds adopt *s-trans* arrangement on carboxy ester and thiophene as predicted from DFT conformational screening on compound **2**. Rotation of pendant phenyl rings with respect to pyrrolinone in compounds **2m** and **4m** strongly depends on crystal packing. While theoretical DFT dihedral angles are 74° for both **2m** and **4m**, the experimental ones cover a wide range from 51° for **2m**, over 72° for **4m**(**b**) to 88° for **4m**(**a**). The calculated exocyclic C═C and C—C bond lenghts in S_0 state are 1.364 Å and 1.456 Å, 1.364 Å and 1.432 Å, 1.367 Å and 1.427 Å for **1m**, **2m**, **4m**, respectively, while the corresponding experimental values are 1.349 Å

Table 3
DFT (S$_0$) and TD DFT (S$_1$) computed exocyclic bond lengths of model compounds **1**, **2** and **4** *without* the side carboxy ester group. Corresponding dihedral C—C=C—C and C=C—C=C angles are in parentheses.

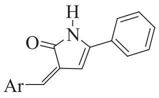

Ar	State	$L_{C=C}$ (Å)	$L_{C–C}$ (Å)
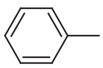	S$_0$	1.364(179°)	1.453 (179°)
	S$_1$	1.409 (180°)	1.423 (179°)
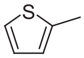	S$_0$	1.364 (180°)	1.432 (179°)
	S$_1$	1.410 (166°)	1.400 (177°)
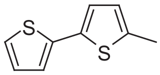	S$_0$	1.367 (180°)	1.427 (179°)
	S$_1$	1.410 (175°)	1.391 (180°)

and 1.465 Å, 1.355 Å and 1.431 Å, 1.351 Å and 1.438 Å (the last ones for **b** molecule of **4m**). DFT calculations thus a bit overestimate the delocalization in the ground electronic state.

As all methylidene-pyrrolinone derivatives in our previous studies (including **1**, **1m** and **3**) [12,16] all five new derivatives **2**, **2m**, **3m**, **4** and **4m** also arose solely as *Z*-isomers from reaction by NMR analysis of their fresh DMSO-d_6 solutions (Table 2). In some cases the rise of the second set of signals corresponding to *E*-isomer was observed (e.g. compound **2** in Table 2). The values of methyl and methylene ^{1}H chemical shifts of all compounds indicate *s-trans* conformation of side carboxy ester group in *Z*-isomers [12], confirmed by X-ray structures for **1m** [12], **2m** and **4m**.

Fluorescence, as the key process in this study, comes (usually) from relaxed lowest excited singlet state. Thus it is of interest to know the geometrical relaxation in S$_1$ compared S$_0$ state, especially with respect to the rigidity on exocyclic parts of the molecules. As the TD DFT excited state geometry optimization require an extreme computing costs, only the model compounds **1**, **2** and **4** *without* the side carboxy ester group were studied. A satisfactory agreement between the experimental and theoretical values of both exocyclic carbon–carbon bond lengths for compounds **1m**, **2m** and **4m** in the ground state implies, that the values for model compounds may be also realistic (Table 3). While these carbon–carbon bond lengths show distinct single and double bond character in S$_0$ state, there is a considerable equalization of their lengths in S$_1$ excited state. The lost of bond lengths alternation, i.e. prolonging of originally double bond, thus opens the *Z*/*E* photoisomerization route. From this point of view there is no difference among the model compounds, as the excited state bond lengths, around which the potential rotation occurs, are the same within 0.001 Å. On the other hand, originally (in S$_0$) single exocyclic carbon–carbon bonds show a dramatic differences in S$_1$. Its length decreases from 1.423 Å for model compound **1** to 1. 1.391 Å for **4**. Furthermore, although the bond lengths of originally double bond are the same for compounds **2** and **4** in S$_1$, there is a remarkably bigger torsion around it for model **2**, as a result of sterical hindrance between S atom and O(=C) atom from pyrrolinone ring. Finally, the key methylidene carbon is fixed in compound **4** considerably more than in other compounds. On assumption, that the excited state rotation around the methylidene-pyrrolinone bond needs a conformational support from its nearest intramolecular neighborhood (e.g. partial rehybridization on methylidene carbon or a partial rotation around the adjacent exocyclic bond), model compound **4** can be considered as the most resistant, because the bonding of exocyclic carbon is the most rigid.

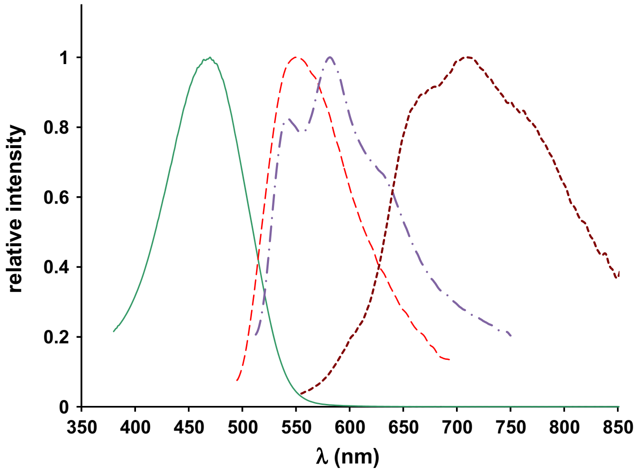

Fig. 3. From the left to right: absorption in DMSO, fluorescence in DMSO, fluorescence in MTHF at 77 K and ss fluorescence of compound **4**.

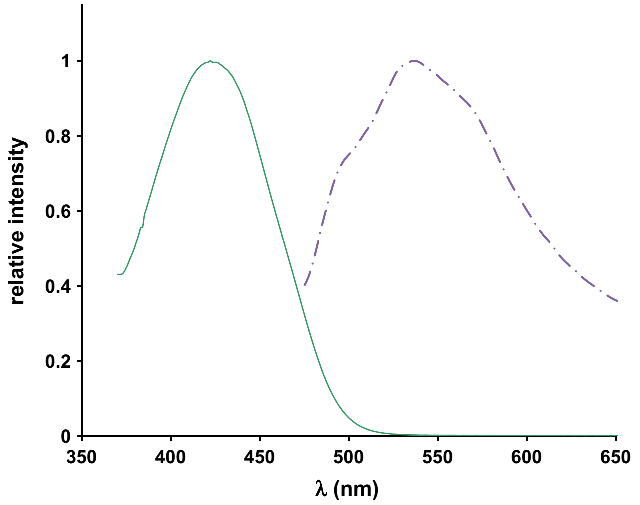

Fig. 4. Absorption in DMSO and fluorescence in MTHF at 77 K of compound **2m**.

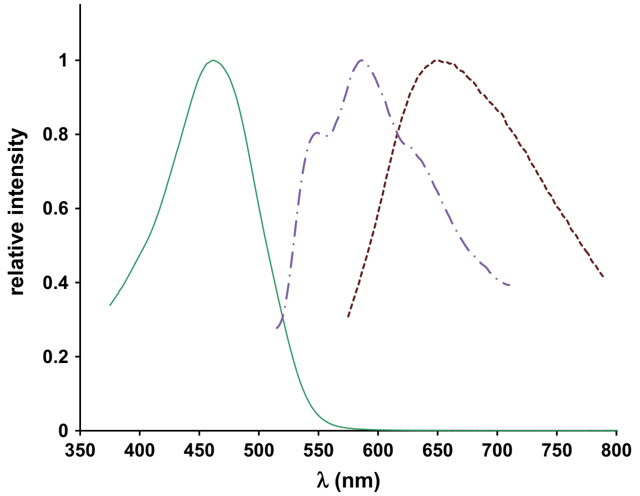

Fig. 5. From the left to right: absorption in DMSO, fluorescence in MTHF at 77 K and ss fluorescence of compound **4m**.

Table 4
Absorption maxima and molar absorptivities in DMSO, fluorescence excitation and emission maxima in MTHF at 77 K and fluorescence maxima in solid state of the compounds under study. The bolded values of ss fluorescence correspond to intense emission, easily detectable by naked eye.

	Abs. DMSO λ_{max} (nm)	Molar Absorp. ε_{max} ($l\ mol\ cm^{-1}$)	Exc. MTHF λ_{max} (nm)	Fluor. MTHF λ_{max} (nm)	Fluor. solid λ_{max} (nm)
1	412	11,900	408	522	–
1m	409	8700	406	535	**561**
2	432	19,500	441	526	544
2m	422	20,100	432	537	–
3	425	16,500	420	538	**606**
3m	421	14,300	430	547	**590**
4	469	52,700	491	582	710
4m	462	33,900	462	587	**651**

Table 5
TD DFT excitation energies recomputed to wavelengths, oscillator strengths and expansion coefficient of the dominating electronic configuration of the first two singlet transitions. Computations were carried out for *Z* isomers/*s-trans* conformers for all compounds.

	S_0–S_1			S_0–S_2		
	λ_{00}	f_{osc}	Coeff.	λ_{00}	f_{osc}	Coeff.
1	431	0.563	0.63 (1–1′)	325	0.018	0.54 (6–1′)
1m	421	0.343	0.62 (1–1′)	326	0.026	0.53 (2–1′)
2	436	0.629	0.70 (1–1′)	331	0.147	0.57 (2–1′)
2m	428	0.417	0.69 (1–1′)	332	0.394	0.67 (2–1′)
3	447	0.914	0.70 (1–1′)	352	0.303	0.67 (2–1′)
3m	438	0.630	0.69 (1–1′)	353	0.586	0.68 (2–1′)
4	496	1.048	0.71 (1–1′)	385	0.070	0.65 (2–1′)
4m	484	0.887	0.70 (1–1′)	389	0.195	0.68 (2–1′)

3.2. Absorption and fluorescence of isolated molecules

The absorption spectra of all compounds under study in DMSO show one structureless band in visible area (Figs. 3–5). The experimental maxima are summarized in Table 4. Visible absorption relates to allowed and strong HOMO–LUMO transition; the second singlet–singlet transition is weak HOMO-1–LUMO and falls into the UV region (Table 5). Theoretical excitation energies are a bit lower with respect to the experimental ones, because the absorption maxima relate to higher vibronic transitions [12]. Both heterosubstitution and conjugation extension brings a bathochromic and hyperchromic shift, while the effect of *N*-methylation is opposite, as predicted.

We have explained the usual absence of fluorescence of methylidene pyrrolinones in solution and its presence in low temperature solvent glass by an effect of environment rigidity hindering the excited state rotation leading to *Z*/*E* isomerization [12,16]. Consequently, all compounds studied here show fluorescence in MTHF glass at 77 K (Figs. 3–5, Table 4), while only the most rigid (in S_1) compound **4**, as supported by TD DFT calculations, but not more distorted compound **4m**, is the only one weakly fluorescent in DMSO solution at room temperature (Figs. 3 and 5).

3.3. Crystal packing and solid-state fluorescence

Common presence of ss fluorescence of all *N*-methylated derivatives was ascribed to the effect of crystal environment rigidity and to an absence of strong intermolecular interactions leading to energy or electron transfers, quenching the fluorescence [12]. From this point of view the intense yellow fluorescence of **1m**, orange fluorescence of **3m** and the red one of **4m** (Fig. 6) were generally

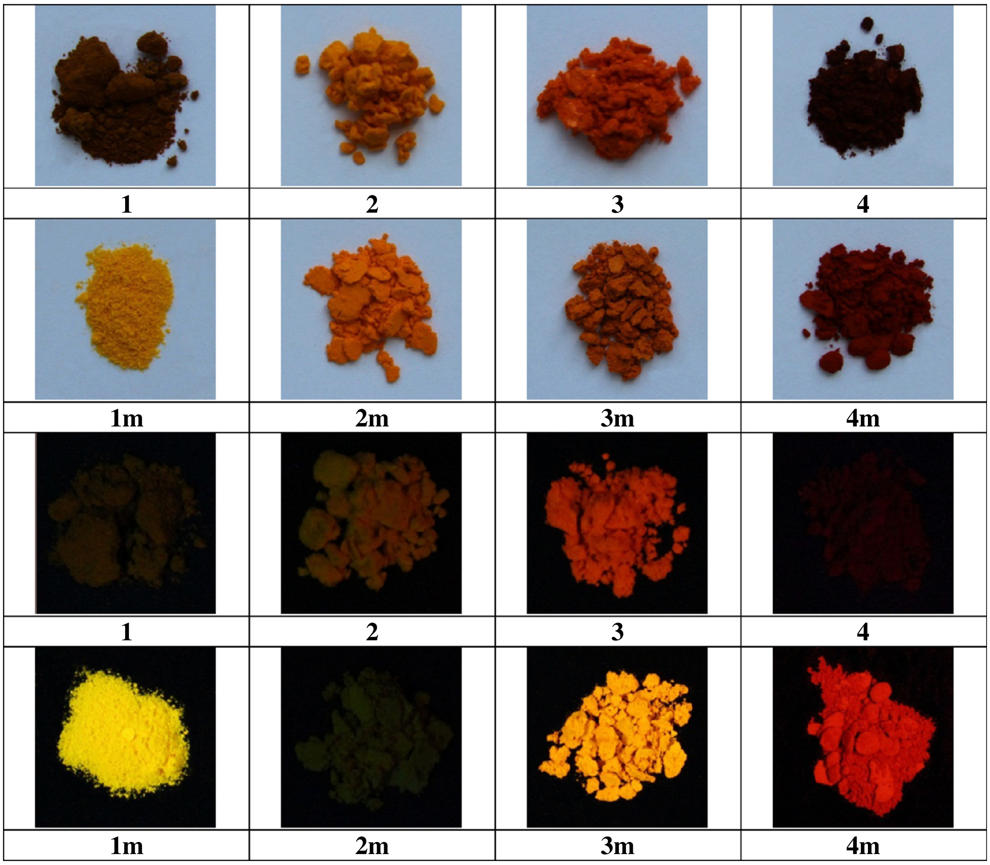

Fig. 6. Polycrystalline samples of **1**–**4m** under daylight (top) and under UV (365 nm) irradiation (bottom).

(a) Compound **1m**

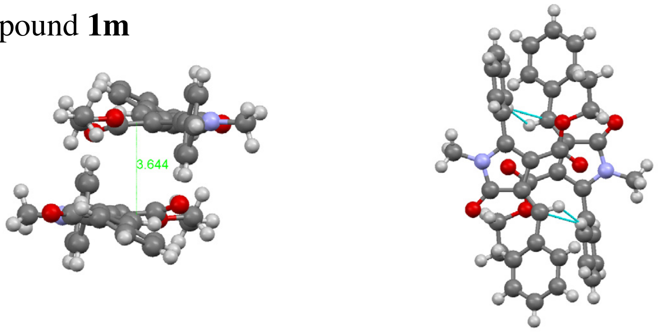

(b) Compound **2m**

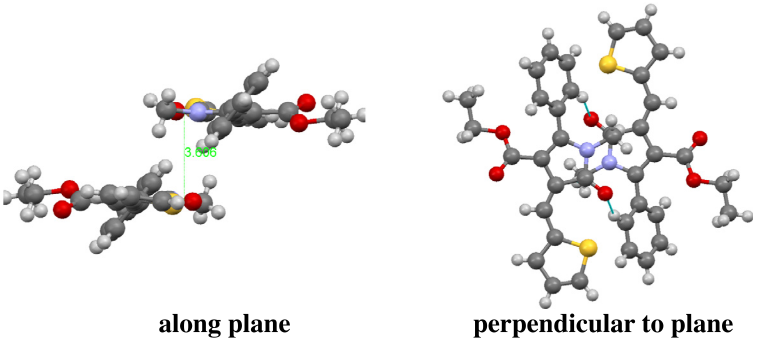

Fig. 7. Crystal packing of **1m** (top) and **2m** (bottom). Molecular planes in dimers are defined by coplanar pyrrolinone rings. Planes are separated 3.644 Å (**1m**) and 3.606 Å (**2m**). Short contacts (less than a sum of van der Waals radii) inside the dimer are pointed out in perpendicular view.

(a) **4m (a)**

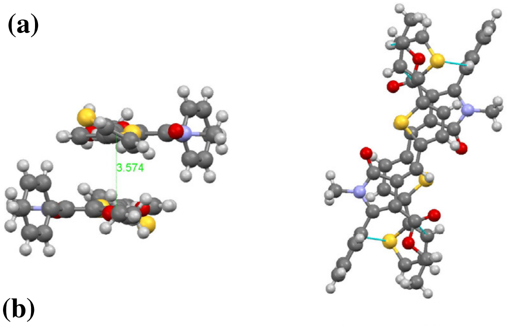

(b) **4m (b)**

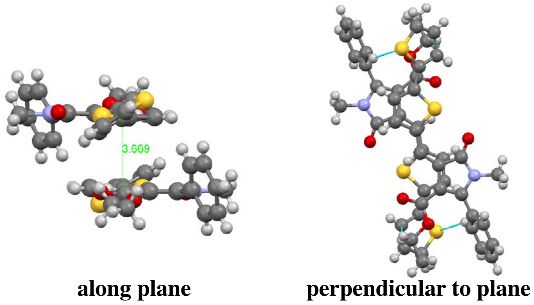

Fig. 8. Crystal packing of **4m** (molecule **a** on top, **b** bottom). Molecular planes in dimers are defined by coplanar pyrrolinone rings. Planes are separated 3.574 Å (**4m(a)**) and 3.669 Å (**4m(b)**). Short contacts (less than a sum of van der Waals radii) inside the dimer are pointed out in perpendicular view.

expected as a consequence of crystal rigidity and a bathochromic shift accompanying the conjugation extension. Relatively strong solid-state fluorescence of compound **3** is exceptional within the series, as its absence is more common for non-alkylated derivatives. We expect the role of non-planar biphenyl part in hindering the quenching intermolecular interactions (transfers), but as the X-ray structure is not on dispose, we will let the nature of this phenomenon open. The main discussion will thus be oriented on unexpected, the first time in a given set observed absence of ss fluorescence of compound **2m**. An interpretation is based on assumption, that excited state out-of-plane rotation as the crucial intramolecular deactivation channel in fluid environment can be hindered in crystal, if the rotating (hetero)aryl-methylidene group is fixed by interplane fixation. In-plane contacts in crystal are considered to be insufficient.

There is a considerable difference between crystal packing of compounds **1m** and **2m** (Fig. 7). Both compounds show no π–π stacking between the adjacent coplanar molecules, so an energy or electron transfer is not efficient. Both exocyclic methylidene carbon and hydrogen atoms in compound **1m** are fixed by two short contacts with respect to out-of-plane torsion in dimer. On the other hand, there is no short contact in dimer of **2m** with a participation of either thiophene or methylidene atoms. Consequently (partial), excited state torsion is not sufficiently hindered in **2m** and ss fluorescence is not observed, on account of non-radiative monomolecular deactivation.

On the contrary to **4**, compound **4m** does not show fluorescence in solution. So it's extremely strong ss fluorescence must come from hindering of excited state torsion in solid-state, but in the same time the quenching by electron or energy transfers must be limited. This situation exactly corresponds with the crystal packing (Fig. 8). Both molecules **a** and **b** of **4m** are strongly interacting in interplanar dimers with respect to bithiophenyl torsion as each of pendant thiophene rings is fixed by three (**4m(a)**) or two (**4m(b)**) out-of-plane short contacts. On the other hand, central coplanar pyrrolinone and thiophene rings of both molecules in both dimers show a minimal π–π stacking, because of a lateral shift and opposite orientation of both molecules.

4. Conclusion

Solid-state fluorophores of methylidene-pyrrolinone type were studied. All compounds fluoresce in low temperature solvent glass as observed in previous studies. There was found an exception from usual solid state photophysical behavior: an absence of strong solid-state fluorescence of *N*-methylated derivative **2m**, which was ascribed to insufficient hindering of methyl-thiophene radical rotation in crystal environment. Generally, our model of photophysical/photochemical behavior remains acceptable: the key excited process is a rotation around the weakened methylidene-pyrrolinone carbon–carbon bond. If this rotation is restricted by rigid environment (always by solvent glass and in most cases in crystal solid-state) and/or excited state bonding, fluorescence is observable. Strong solid-state fluorescence of *N*-methylated derivatives shows a bathofluoric shift 90 nm when going from parent **1m** to **4m**, which fluorescence maximum (651 nm) is at the longest wavelength ever observed for methylidene-pyrrolinones.

Appendix A. Supplementary material

Supplementary data associated with this article can be found, in the online version, at http://dx.doi.org/10.1016/j.molstruc.2013.03.051.

References

[1] M. Shimizu, T. Hiyama, Chem. Asian J. 5 (2010) 1516.
[2] M.B. Smith, J. Michl, Chem. Rev. 110 (2010) 6891.
[3] S.-Y. Park, M. Ebihara, Y. Kubota, K. Funabiki, M. Matsui, Dyes Pigm. 82 (2009) 258.
[4] S.-Y. Park, Y. Kubota, K. Funabiki, M. Shiro, M. Matsui, Tetrahedron Lett. 50 (2009) 1131.
[5] M. Matsui, R. Ikeda, Y. Kubota, K. Funabiki, Tetrahedron Lett. 50 (2009) 5047.
[6] Y.-N. Yan, W.-I. Pan, H.-C. Song, Dyes Pigm. 86 (2010) 249.
[7] Y.-F. Sun, S.-H. Xu, R.-T. Wu, Z.-Y. Wang, Z.-B. Zheng, J.-K. Li, Y.-P. Cui, Dyes Pigm. 87 (2010) 109.
[8] Ch. Kitamura, H. Tsukuda, A. Yoneda, T. Kawase, T. Kobayashi, H. Naito, Eur. J. Org. Chem. (2010) 3033.
[9] H. Langhals, T. Potrawa, H. Nöth, G. Linti, Angew. Chem. Int. Edit. 28 (1989) 478.
[10] J. Plötner, A. Dreuw, Phys. Chem. Chem. Phys. 8 (2006) 1197.
[11] Y. Jin, Y. Xu, Y. Liu, L. Wang, H. Jiang, X. Li, D. Cao, Dyes Pigm. 90 (2010) 311.
[12] S. Luňák Jr., Z. Eliáš, J. Vyňuchal, A. Lyčka, Z. Padělková, R. Hrdina, J. Mol. Struct. 1022 (2012) 159.
[13] S. Luňák Jr., M. Vala, J. Vyňuchal, I. Ouzzane, P. Horáková, P. Možíšková, Z. Eliáš, M. Weiter, Dyes Pigm. 91 (2011) 269.
[14] A.B. Tamayo, M. Tantiwiwat, B. Walker, T.Q. Nguyen, J. Phys. Chem. C 112 (2008) 15543.
[15] S. Luňák Jr., L. Havel, J. Vyňuchal, P. Horáková, J. Kučerík, M. Weiter, R. Hrdina, Dyes Pigm. 85 (2010) 27.
[16] J. Vyňuchal, S. Luňák Jr., A. Hatlapatková, R. Hrdina, A. Lyčka, L. Havel, K. Vyňuchalová, R. Jirásko, Dyes Pigm. 77 (2008) 266.
[17] Z. Otwinowski, W. Minor, Methods Enzymol. 276 (1997) 307.
[18] P. Coppens, in: F.R. Ahmed, S.R. Hall, C.P. Huber (Eds.), Crystallographic Computing, Munksgaard, Copenhagen, 1970, pp. 255–270.
[19] A. Altomare, G. Cascarano, C. Giacovazzo, A. Guagliardi, J. Appl. Crystallogr. 26 (1993) 343.
[20] G.M. Sheldrick, SHELXL-97, University of Göttingen, Göttingen, 1997.
[21] M.J. Frisch, G.W. Trucks, H.B. Schlegel, G.E. Scuseria, M.A. Robb, J.R. Cheeseman, G. Scalmani, V. Barone, B. Mennucci, G.A. Petersson, H. Nakatsuji, M. Caricato, X. Li, H.P. Hratchian, A.F. Izmaylov, J. Bloino, G. Zheng, J.L. Sonnenberg, M. Hada, M. Ehara, K. Toyota, R. Fukuda, J. Hasegawa, M. Ishida, T. Nakajima, Y. Honda, O. Kitao, H. Nakai, T. Vreven, J.A. Montgomery Jr, J.E. Peralta, F. Ogliaro, M. Bearpark, J.J. Heyd, E. Brothers, K.N. Kudin, V.N. Staroverov, R. Kobayashi, J. Normand, K. Raghavachari, A. Rendell, J.C. Burant, S.S. Iyengar, J. Tomasi, M. Cossi, N. Rega, J.M. Millam, M. Klene, J.E. Knox, J.B. Cross, V. Bakken, C. Adamo, J. Jaramillo, R. Gomperts, R.E. Stratmann, O. Yazyev, A.J. Austin, R. Cammi, C. Pomelli, J.W. Ochterski, R.L. Martin, K. Morokuma, V.G. Zakrzewski, G.A. Voth, P. Salvador, J.J. Dannenberg, S. Dapprich, A.D. Daniels, O. Farkas, J.B. Foresman, J.V. Ortiz, J. Cioslowski, D.J. Fox, Gaussian 09, Revision A.1, Gaussian, Inc., Wallingford CT, 2009.